A Detailed Balance Study of Rear Surface of $Cs_3Sb_2Br_9$ Perovskite Solar Cell

Sachchidanand[1], Akash Patnaik[1], Anil Kumar[2], Pankaj Sharma[1,*]

[1] Advanced Semiconductor Materials and Nanoelectronics (ASMAN) Research Group, Indian Institute of Information Technology, Design and Manufacturing, Jabalpur (India)

[2] Department of Electronics and Communication Engineering, PDPM Indian Institute of Information Technology, Design and Manufacturing, Jabalpur (India)

Abstract

An analytical model based on a detailed balance theory has been adopted to obtain the performance limitation of a $Cs_3Sb_2Br_9$-based perovskite solar cell (PSC). Two different structures surrounded by the angular reflection layer at the front along with a perfect mirror and an absorbing substrate at the rear surface, individually, are investigated. The performance analysis of both structures on the cell is done by tuning the angle of incident sunlight. The obtained result highlights an increment of 1.6% in the performance for the perfect mirror-based structure as compared to the other structure. The obtained result signifies a good performance of the $Cs_3Sb_2Br_9$-based PSC for a plane wave (90°). The proposed analytical model and corresponding results can be used as a suitable model for estimating the performance parameters of the PSC for various materials.

Keywords: $Cs_3Sb_2Br_9$, perovskite solar cell, detailed balance model, AM1.5G, absorbing substrate, perfect mirror

1. Introduction

Solar cells (SCs) are the most attractive technology in recent years due to a very vast range of emerging materials that drastically improve the device's performance. For decades, emerging perovskite materials have attracted the solar community for a low-cost device with reliable performance. The recent reports on perovskite-based SCs (PSCs) with the highest efficiency of 26.1% encourage the research community ((NREL), n.d.; Green et al., 2023). Moreover, the large range of perovskite materials and cost-effective fabrication methods like solution-based methods, sol-gel, hot-injection, etc. also support the development of efficient PSCs (Shah et al., 2020). Firstly, Sha et al. proposed a detailed balance model to calculate the efficiency limit of $CH_3NH_3PbI_3$ PSCs and calculated the limit as 31% (Sha et al., 2015). Sun et al. approached a physics-based analytical model of PSCs using a fitting function (Sun et al., 2015). Agarwal et al. proposed a scheme of device engineering to achieve a nearly ideal efficiency of PSC (Agarwal and Nair, 2015). Ren et al. explored the drift-diffusion-based analytical model for obtaining the theoretical limit of PSC (Ren et al., 2017). In the context of a lead-free perovskite, we have designed a $Cs_3Sb_2Br_9$-based PSC and all-perovskite tandem solar cell (TSC), for the first time, to determine the contribution of $Cs_3Sb_2Br_9$ in these devices (Sachchidanand et al., 2023, 2022, 2021). This work presents a detailed balance model-based analytical approach on $Cs_3Sb_2Br_9$-based PSC to study the performance limit of the cell (PSC).

2. Model development

To do an investigation, two different structures are proposed, as shown in Fig. 1. For Fig. 1(a) the optical medium surrounding the photovoltaically active absorbing cell is "air" at the front surface and a perfect reflector mirror at the rear surface. Any solar cell thick enough to be manufactured with the back surface of its

10.18086/swc.2023.01.05 Available at http://proceedings.ises.org

active region accessible to make it a perfect reflector can possibly approach such a device. For Fig. 1(b) the absorbing cell is surrounded by "air" at the front surface and an absorbing substrate at the rear surface. Such a structure emphasises a more practical situation that is highly adopted in fabricating any solar cell. The Assuming only the radiative recombination mechanism exists, under illumination at the steady state condition, photon absorption in the cell must be equal to the photon emission, corrected for the fraction *f* as current in the external circuit.

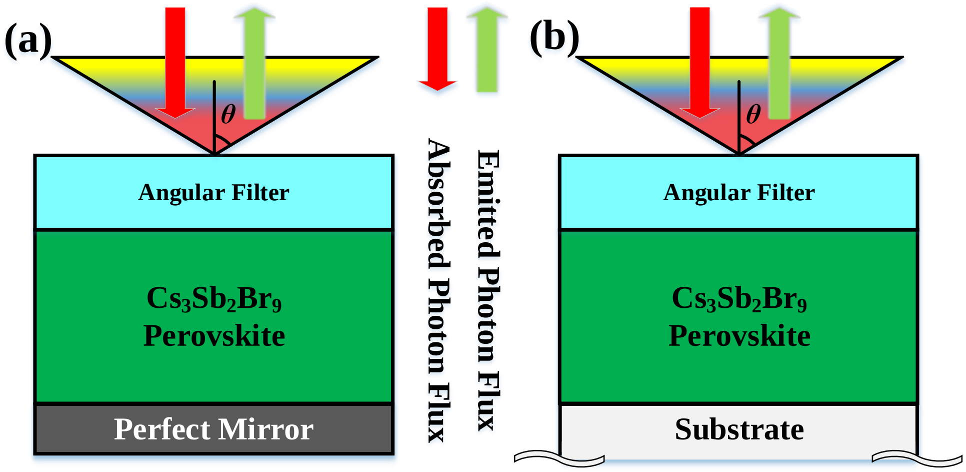

Fig. 1 Schematic of $Cs_3Sb_2Br_9$-based perovskite solar cell (PSC). The structure has a planar top surface along with (a) a perfect mirror, and (b) an absorbing substrate at the rear surface.

$$J_0 exp\left(\frac{qV}{kT}\right) = (1-f)J_L \quad \text{(eq. 1)}$$

The photogenerated current (J_L) after photon absorption can be computed as:

$$J_L = \frac{q}{hc}\int_0^\infty \Gamma(\lambda)a(\lambda)\lambda d\lambda \quad \text{(eq. 2)}$$

where $\Gamma(\lambda)$ is the incident AM1.5G solar spectrum, $a(\lambda)$ is the absorptivity, q is the electron charge, h is the plank constant, and c is the light speed. The leakage current (J_0) owing to carrier loss can be computed as:

$$J_0 = \frac{q}{hc}\int_0^\infty b(\lambda)a(\lambda)\lambda d\lambda \quad \text{(eq. 3)}$$

where $b(\lambda)$ is the black-body emission spectrum of the cell which can be calculated by (Sha et al., 2015) with consideration of the Boltzmann approximation. Moreover, in a detailed balance model, the maximum current that can circulate through the given external circuit is calculated as the difference between the photogenerated current after photon absorption and leakage current owing to photon emission.

$$J(V) = J_0 exp\left(\frac{qV}{kT}\right) - J_L \quad \text{(eq. 4)}$$

Furthermore, the absorptivity expresses in Eqs. (2) and (3) for both structures depends majorly upon the cell's thickness (W), refractive index (n) and angle of incident sunlight (θ) and can be computed as:

$$a(\lambda) = 1 - exp\left(\frac{-\mathrm{m}\alpha(\lambda)W}{cos(\theta_{inc})}\right) \quad \text{(eq. 5)}$$

Here m is an optical path multiplier owing to the rear surface of the cell; m = 2 for the perfect mirror, and m = 1 for the back absorbing substrate at the rear surface of the cell. $\theta_{inc} = cos^{-1}\left(\sqrt{1-n^{-2}sin^2(\theta)}\right)$ is the angle of propagation inside the absorbing cell after suffering from reflection.

The fixed point performance parameters, short-circuit current density (J_{sc}) and open circuit voltage (V_{oc}), can be obtained from Eq. (4) by putting null to either biasing voltage (V) or current density (J) and can be written as:

$$J_{sc} = -J_L \text{ , and } V_{oc} = V_t ln\left(\frac{J_L}{J_0}\right) \quad \text{(eq. 6)}$$

where $V_t = kT/q$ is the thermal voltage. For an efficient PSC, the power conversion efficiency (PCE) expresses the conversion performance of the cell and can be given by:

$$PCE = \frac{max(J \times V)}{P_L} \quad \text{(eq. 7)}$$

where P_L is AM1.5G spectrum having a power density of 100 mW/cm^2.

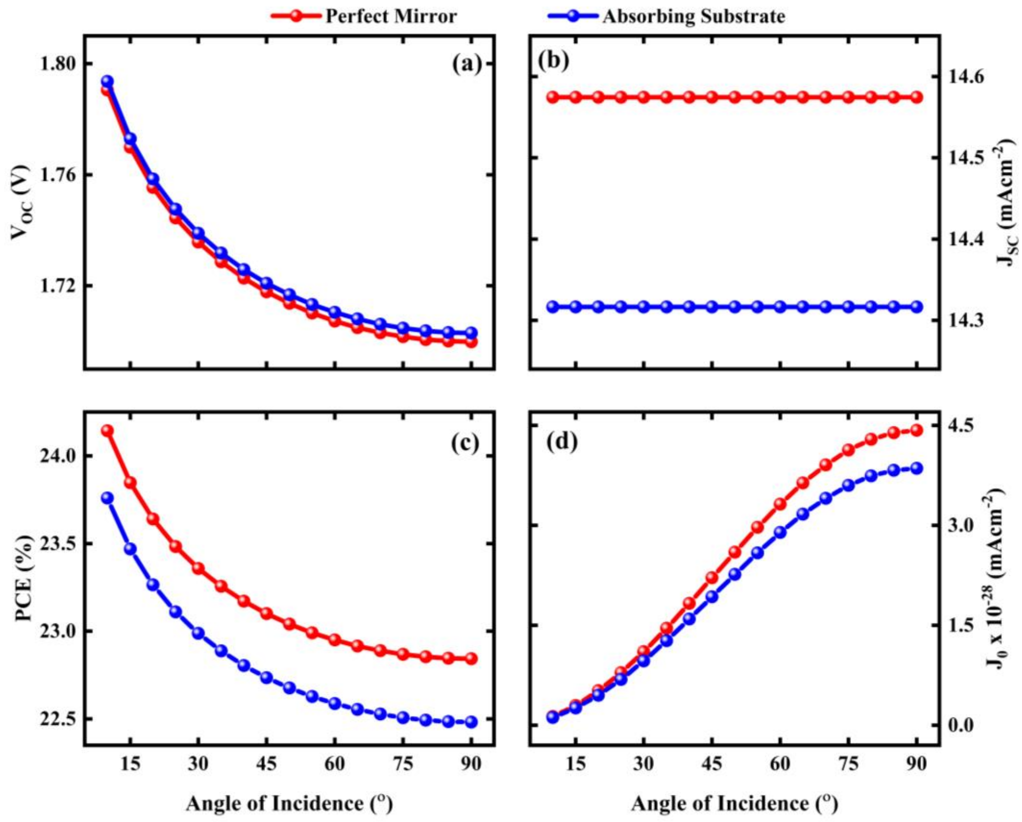

Fig. 2 Performance parameters of both Planar PSCs by varying the incident angle, such as (a) open-circuit voltage (V_{OC}), (b) short-circuit current density (J_{SC}), (c) power conversion efficiency (PCE), and (d) Leakage current density (J_0).

3. Results and discussion

3.1. Influence of rear substrate on the solar incidence angle on structures

In Fig. 2, the influence of solar incidence angle on the performance of the planar structures having perfect mirror and back absorbing substrates is observed. From Fig. 1, the angular restriction layer allows the incident photon to penetrate inside the structure owing an angle of incidence (θ) and bound it's emission. The variations in θ between 10º and 90º having stepping of 5º is depicted in Fig. 2 using V_{OC}, J_{SC}, PCE and J_0. As θ increases the V_{OC} decreases and J_0 increases exponentialy with a marginal difference for both structures at $\theta > 30$º. This variation in V_{OC} and J_0 is due to rise in the direct recombination of photon because of a rise in the angle of emission which is the counterpart of θ (Ren et al., 2017). Moreover, as θ gets updated, J_{SC} accounts a fixed value with a 0.61% higher value for the structure having the perfect mirror on the rear side{Fig. 1(a)} instead of that of the back absorbing substrate {Fig. 1(b)}. This fixed J_{SC} may be due to the constant generation of free charge carrier at thermal equilibrium and the difference is due to the different optical path of the free charge carriers in both structures (Sachchidanand et al., 2022; Sun et al., 2015). As PCE is the effective performance of the structure which can be calculated as the ratio of the maximum value of the multiplication of current density J and baised voltage V to the incident solar power (P_L), as in Eq. (7). From Fig. 2(c), as θ changes, the performance of both structures varies which follow the nature of V_{OC} because of fixed J_{SC}. The planar structure having the perfect mirror shows a better outcome in comparison to the planar structure having the back absorbing substrate due to double absorptivity hence better J_{SC}, see Fig. 2(b). Thus, it can be concluded that the $Cs_3Sb_2Br_9$-based PSC having the perfect mirror performed well with a 1.6% higher PCE in comparison to that structure having the back absorbing substrate. Table 1 displayed a performance comparison of $Cs_3Sb_2Br_9$-

based PSC with previous detailed balance-based models and experimental reports.

Tab. 1: Performance comparison of $Cs_3Sb_2Br_9$-based PSC with previous detailed balance-based model and experimental reports

Perovskite	E_g (eV)	Angle of Incidence (°)	PCE (%)	
			Detailed Balance-based Model	Experimental
$MAPbI_3$	1.5	90	28.82 (Sha et al., 2015)	25.50 (Li et al., 2021)
$MAPbBr_3$	2.2	90	19.60 (Shockley and Queisser, 1961)	4.85 (Mehdi et al., 2019)
$Cs_3Sb_2Br_9$	2.0	90	22.84 [This Work]	-

3.2. Impact of solar incidence angle on structures with different front design

An investigation of the performance of the 'Planar Front' and 'Textured Front' based PSC is presented in Fig. 3(a) as the function of θ. In both PSCs, as θ increases, the performance starts decay which may be due to decrease in the absorptivity which increases the recombination of charge carriers in the structure (Rühle, 2016). Moreover, the effect of different absorber's thickness like 800 nm, 1000 nm, and 1200 nm on both PSCs is also depicted in Fig. 3(a). The 'Planar Front' PSC shows a negligible difference by varying the absorber's thickness may be due to double optical path. While the 'Textured Front' PSC shows a difference of 1.15% and 1.83% for the absorber thickness of 1000 nm and, 1200 nm in compared to that of 800 nm, respectively. These marginal differences in the PSC may be due to lesser emission of the incident photon at the higher thicknesses of the absorber. As result, the 'Planar Front' and the 'Textured Front' PSCs reaches a maximum PCE of 22.84% and 22.48%, respectively, at θ of 90° and the absorber thickness of 1000 nm. This may also be due to lower optical path of the charge carriers at the front texturing design in compared to front planar design. It highlights the elevated performance of the 'Planar Front' PSC and concluded the optimum absorber thickness of 1000 nm. The influence of different front design and back substrate at the absorber thickness of 1000 nm is depicted in Fig. 3(b). It shows a maximum performance limit of 24.14% at θ of 10° for the $Cs_3Sb_2Br_9$-based PSC having planar front and back mirror design. Thus for a lead-free inorganic $Cs_3Sb_2Br_9$-based PSC, the maximum performance is achieved for a 'Planar Front' having a back mirror design.

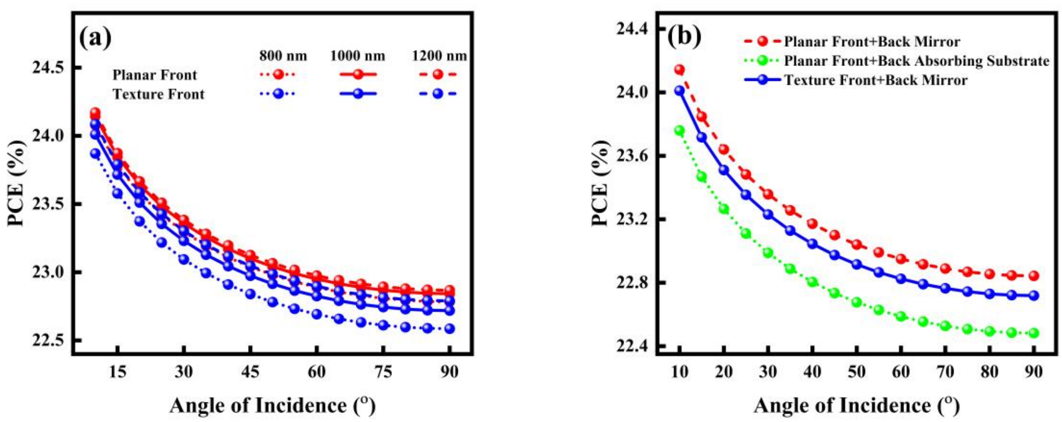

Fig. 3 Variation in the power conversion efficiency (PCE) of (a) the planar and texture front having a back perfect mirror at different thicknesses of 800 nm, 1000 nm, and 1200 nm, and (b) different structures at the thickness of 1000 nm as the function of angle of incidence.

4. Conclusion

A detailed balance model-based analytical approach for the calculation of the performance limit of $Cs_3Sb_2Br_9$-based PSC is investigated. The variation in the performance parameters as the function of the angle of incident sunlight is observed. The obtained result highlights that the perfect mirror-based structure reflected a better performance limited of 22.84% at θ of 90° which is 1.6% higher as compared to the back absorbing structure.

It also signifies that for a good performance of the $Cs_3Sb_2Br_9$-based PSC, a perfect mirror helps to improve the performance by increasing the optical path and lowering the photon emission angle. The discussed analytical model and its corresponding result can be used as a suitable model for estimating the performance-limiting parameters of the PSC for various materials.

5. Acknowledgments

The author would like to thank Dr. Anil Kumar for his keen support in the research and also acknowledge Dr. Pankaj Sharma for providing Faculty Initiation Grant no. IIITDMJ/Dir. Off. /109/2020/11/41. This work is partially supported by DST Science & Engineering Research Board (SERB) project no. SRG/2021/001946.

6. References

(NREL), N.R.E.L., n.d. best-research-cell-efficiencies-rev220126.pdf.

Agarwal, S., Nair, P.R., 2015. Device engineering of perovskite solar cells to achieve near ideal efficiency. Appl. Phys. Lett. 107. https://doi.org/10.1063/1.4931130

Green, M.A., Dunlop, E.D., Siefer, G., Yoshita, M., Kopidakis, N., Bothe, K., Hao, X., 2023. Solar cell efficiency tables (Version 61). Prog. Photovoltaics Res. Appl. 31, 3–16. https://doi.org/10.1002/PIP.3646

Li, D., Zhang, D., Lim, K.S., Hu, Y., Rong, Y., Mei, A., Park, N.G., Han, H., 2021. A Review on Scaling Up Perovskite Solar Cells. Adv. Funct. Mater. 31, 1–27. https://doi.org/10.1002/adfm.202008621

Mehdi, H., Mhamdi, A., Hannachi, R., Bouazizi, A., 2019. MAPbBr3 perovskite solar cells: Via a two-step deposition process. RSC Adv. 9, 12906–12912. https://doi.org/10.1039/c9ra02036e

Ren, X., Wang, Z., Sha, W.E.I., Choy, W.C.H., 2017. Exploring the Way to Approach the Efficiency Limit of Perovskite Solar Cells by Drift-Diffusion Model. ACS Photonics 4, 934–942. https://doi.org/10.1021/acsphotonics.6b01043

Rühle, S., 2016. Tabulated values of the Shockley-Queisser limit for single junction solar cells. Sol. Energy 130, 139–147. https://doi.org/10.1016/j.solener.2016.02.015

Sachchidanand, Garg, V., Kumar, A., Sharma, P., 2021. Numerical simulation of novel lead-free Cs3Sb2Br9 absorber-based highly efficient perovskite solar cell. Opt. Mater. (Amst). 122, 111715. https://doi.org/10.1016/j.optmat.2021.111715

Sachchidanand, Kumar, A., Sharma, P., 2023. Transfer matrix method-based efficiency enhancement of lead-free Cs3Sb2Br9 perovskite solar cell. Sol. Energy 259, 63–71. https://doi.org/10.1016/j.solener.2023.05.014

Sachchidanand, Kumar, A., Sharma, P., 2022. Performance Investigation of Organic/Inorganic Bottom Cell on Lead-Free Cs3Sb2Br9 Based All-Perovskite Tandem Solar Cell. IEEE Trans. Electron Devices 69, 3462–3469. https://doi.org/https://doi.org/10.1109/TED.2022.3167965

Sha, W.E.I., Ren, X., Chen, L., Choy, W.C.H., 2015. The efficiency limit of CH3NH3PbI3 perovskite solar cells. Appl. Phys. Lett. 106. https://doi.org/10.1063/1.4922150

Shah, S.A.A., Sayyad, M.H., Khan, K., Guo, K., Shen, F., Sun, J., Tareen, A.K., Gong, Y., Guo, Z., 2020. Progress towards High-Efficiency and Stable Tin-Based Perovskite Solar Cells. energies Rev. 13, 1–42. https://doi.org/10.3390/en13195092

Shockley, W., Queisser, H.J., 1961. Detailed balance limit of efficiency of p-n junction solar cells. J. Appl. Phys. 32, 510–519. https://doi.org/10.1063/1.1736034

Sun, X., Asadpour, R., Nie, W., Mohite, A.D., Alam, M.A., 2015. A Physics-Based Analytical Model for Perovskite Solar Cells. IEEE J. Photovoltaics 5, 1389–1394. https://doi.org/10.1109/JPHOTOV.2015.2451000